PERGAMON

Applied Geochemistry 15 (2000) 439–454

Applied Geochemistry

The influence of water–rock interaction on the chemistry of thermal springs in western Canada

Stephen E. Grasby[a,*], Ian Hutcheon[a], H.R. Krouse[b]

[a]*Department of Geology and Geophysics, The University of Calgary, Calgary, Alta., Canada*
[b]*Department of Physics and Astronomy, The University of Calgary, Calgary, Alta., Canada*

Received 22 June 1998; accepted 29 June 1999
Editorial handling by Y. Kharaka

Abstract

A comparison of new data with historical records indicates that the chemistry of thermal springs from the Canadian Cordillera is constant through time, suggesting that water compositions develop equilibrium with the host rock. A thermodynamic model is used to evaluate the influence of water–rock interaction on the chemistry of thermal spring waters. An isotope mass-balance approach is used to evaluate biological controls on the S and C cycles in the springs.

A comparison of mineral stability with water compositions suggests that the activities of major cations are controlled by equilibrium reactions with common rock forming minerals and alteration products. Sulfur has a complex redox history in thermal springs. Sulfate derived from dissolution of evaporite minerals is reduced by bacteria, causing the production of HS^-. The loss of HS^- from the system appears to be minor, instead it is reoxidized to SO_4 as the spring water ascends to surface. Calculations indicate that the amount of SO_4 that is reduced and reoxidized varies from 0 to 53%. There is an inverse relationship between the proportion of biological cycling of SO_4 and the concentration of SO_4, indicating that SO_4 is not a limiting nutrient in hydrothermal systems. In low alkalinity thermal springs, HCO_3 is derived from either dissolution of carbonate minerals or oxidized organic matter. However, for high alkalinity springs (>100 mg/l) HCO_3 is dominantly derived from carbonate dissolution.

1. Introduction

In western Canada, the deep circulation of meteoric waters is thought to have played a significant role in the precipitation of hydrothermal Ag–Au–Pb–Zn deposits and vein forming minerals. Many models of ore formation suggest that reduced S is brought to depth by deep circulating meteoric water, that then mixes with mineralising fluids leading to precipitation of sulfide minerals at depths as great as 5 km (e.g. Nesbitt et al., 1989; Beaudoin et al., 1992; Nesbitt and Muehlenbachs, 1995). Deep circulation of sulfide-rich water occurs in the present day, as shown by the numerous S-rich thermal springs in the Canadian Cordillera. These hydrothermal systems may be forming modern day equivalents to the ore bodies now exposed at the surface. Clearly then, a better understanding of processes controlling the chemistry of mod-

* Corresponding author. Present address: Geological Survey of Canada, Calgary, 3303 33rd St. N.W., Calgary, Alta., Canada T2L-2A7.

E-mail address: sgrasby@gsc.nrcan.gc.ca (S.E. Grasby).

0883-2927/00/$ - see front matter
PII: S0883-2927(99)00066-9

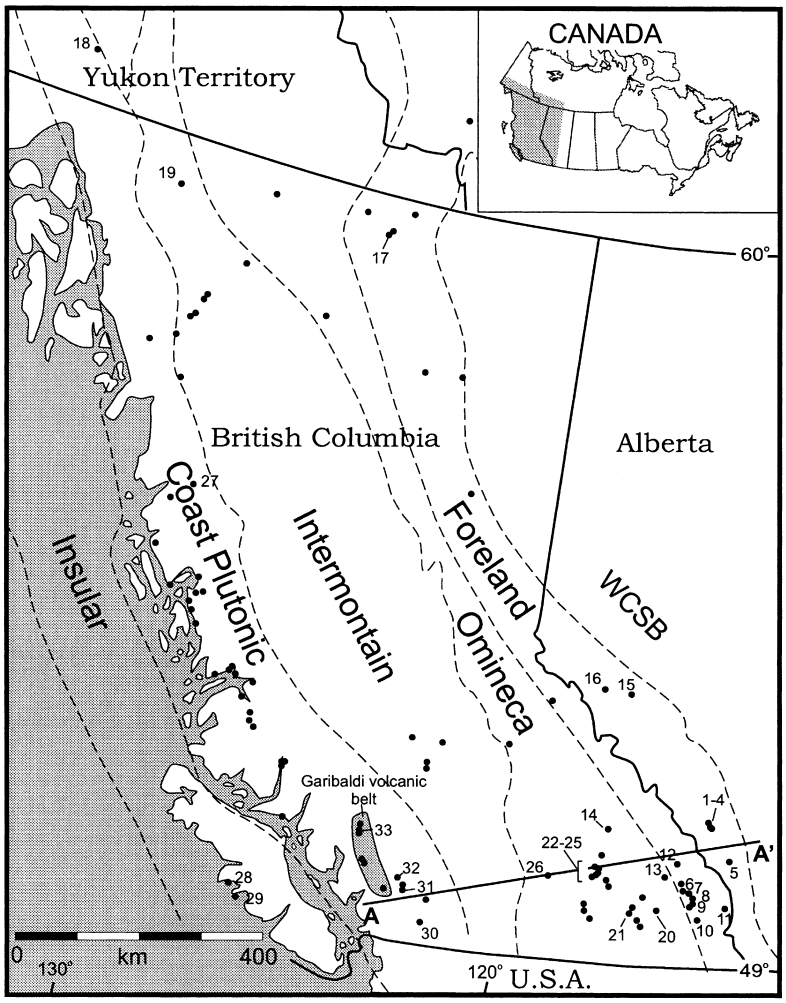

Fig. 1. Regional map of western Canada showing location of known thermal springs and the 5 geomorphological belts of the Canadian Cordillera [after Gabrielse and Yorath (1991)]. Profile A–A′ indicates the transect of Yonge et al. (1989) in Fig. 3. Numbered springs are those sampled in this study, names are given in Table 2. WCSB = western Canada sedimentary basin.

ern thermal springs, and in particular the S cycle in thermal springs, will aid in the refinement of hydrothermal ore-deposit models.

In this study new chemical data is presented and compared with historical records to investigate the consistency of chemical compositions through time of individual thermal springs in western Canada. Consistency of composition would suggest that the chemistry of thermal spring waters is controlled by water–rock interaction, similar to the suggestion of Garrels and Mackenzie (1967). To investigate the underlying controls, the authors use a thermodynamic model to evaluate how water–rock interaction may be controlling the chemistry of thermal spring waters. In addition, an isotope mass-balance approach is used to evaluate biological controls on the S and C cycles in the circulation system. There are over 130 thermal springs in western Canada (Fig. 1); however, many are remote and widely spaced, making access difficult. For this study samples were collected from 33 thermal springs that were chosen to represent a wide geographical area and a range of host rocks.

2. Regional geological setting

The Canadian Cordillera developed in response to the collision of island arc terranes against the western margin of North America from Jurassic to Tertiary (Gabrielse and Yorath, 1991). The Cordillera is divided into 5 morphogeological belts (Fig. 1). These can be roughly defined as deformed sedimentary strata of either North American (Foreland belt) or island arc affinity (Insular and Intermontane belts) that are separ-

Table 1
Chemical analysis for selected thermal springs, illustrating the consistency in chemistry through time. HSC = Hot Springs Cove

Spring	Year	T (°C)	Ca (mg/l)	Mg (mg/l)	Na (mg/l)	K (mg/l)	SiO_2 (mg/l)	SO_4 (mg/l)	Cl (mg/l)	HCO_3 (mg/l)
HSC	1898[a]	52	20	1.0	137	2.0	59.0	35	217	–
HSC	1975[b]	51	18	0.1	141	2.0	53.0	36	206	22
HSC	1990[c]	52	22	0.1	149	2.0	51	31	224	39
HSC	1994[d]	59	18	0.1	143	2.0	37.0	36	221	21
Banff Cave	1916[e]	30	1028	39.2	6.0	4.5	23.4	580	10.0	140
Banff Cave	1967[f]	31	1015	42.8	5.1	3.8	27.0	559	5.0	153
Banff Cave	1994[d]	30	1208	45.9	5.5	4.5	27.0	696	5.4	126
Lussier	1968[f]	43	145	25.0	875	10.0	36.0	135	1402	218
Lussier	1993[d]	43	115	24.8	979	10.6	36.6	148	1400	222
Ram Creek	1968[f]	35	50.0	15.0	2.6	1.3	21.0	57.0	1.2	155
Ram Creek	1993[d]	37	49.2	14.5	2.4	1.3	21.3	56.0	1.2	148
Fairmont	1967[f]	49	472	112	31.0	5.6	37.9	990	41.9	699
Fairmont	1993[d]	47	451	107	29.0	5.5	32.9	929	34.0	685
Radium	1967[f]	43	142	28.3	15.0	2.8	36.0	302	9.2	212
Radium	1993[d]	44	150	33.2	14.9	3.3	38.6	356	13.2	217
Takhini	1961[g]	43	594	86.5	40.0[*]		35.0	1684	4.0	138
Takhini	1976[h]	47	575	75	34	8.2	98	1768	1.5	65
Takhini	1994[d]	46	611	79.2	35.1	8.8	89.1	1670	1.0	112

[a] Clapp (1913).
[b] Souther and Halstead (1973).
[c] Phillips (1994).
[d] This study.
[e] Elworthy (1918).
[f] van Everdingen (1972).
[g] Wheeler (1961).
[*] = (Na + K).
[h] Crandall and Sadlier-Brown (1976).

ated by welts of plutonic and high-grade metamorphic rocks (Coast and Omenica belts). Compressional deformation ended abruptly in the southern Cordillera during the Eocene. At this time crustal-scale extension faults formed in the SE Cordillera, with associated plutonism and volcanism (Armstrong, 1988; Gabrielse and Yorath, 1991). From Eocene to recent, the SW Cordillera has been affected by right-lateral strike-slip faulting. In addition, the Garibaldi volcanic belt developed from late Tertiary to Quaternary (Fig. 1) (Lewis and Souther, 1978).

3. Methodology

White (1975) defines thermal springs as ground water discharge >5°C above local mean annual air temperature. For the purpose of this paper, 4°C is used as an average air temperature, restricting the study to springs with discharge temperature above 9°C. In many locations, several closely spaced springs occur within tens of metres of each other. In these cases, it is assumed that a group of springs represents a single hydrothermal system and that the hottest outlet represents the least amount of mixing with shallow ground water. Thus, locations with several closely spaced springs are represented by a sample of the hottest outlet. Generally, water samples were collected less than 1 m from the rock face that forms the outlet. At Radium Hot Springs 4 closely spaced springs are piped to a sump, where a bulk sample was collected.

Unstable parameters (pH, temperature, Eh, dissolved O_2, and HS^-) were measured in situ. Dissolved O_2 and HS^- were measured using Chemetrics® colorimetric kits. For the remaining analyses, samples were collected and preserved in the field. The water was passed through a 0.45 μm filter. Samples for cation analysis were acidified to pH < 2 with ultrapure HNO_3. Samples for anion analysis were untreated and stored at 4°C. For SiO_2 determination, 10 ml of sample were diluted in the field with 50 ml of doubly distilled water. Sample bottles were cleaned following procedures defined by Environment Canada (1983).

For stable isotope analysis, dissolved sulfide was precipitated in the field by the addition of Cd acetate and samples were stored in the dark. Within a week of collection, the CdS precipitate was filtered and reacted with $AgNO_3$ to form Ag_2S. Dissolved SO_4 was then

Table 2
Chemical and stable isotope analyses for thermal springs in this study. N/A refers to species not present, (–) refers to species not analysed

Location	No.	T (°C)	pH	$\delta^{34}S_{SO_4}$ (‰)	$\delta^{34}S_{H_2S}$ (‰)	$\delta^{18}O_{SO_4}$ (‰)	δD_{H_2O} (‰)	$\delta^{18}O_{H_2O}$ (‰)	$\delta^{13}C_{HCO_3}$ (‰)	O_2 (mg/l)	TDS (mg/l)	HCO_3 (mg/l)	SO_4 (mg/l)	H_2S (mg/l)	Cl (mg/l)	NO_3 (mg/l)	SiO_2 (mg/l)	Ca (mg/l)	Mg (mg/l)	Na (mg/l)	K (mg/l)	Sr (mg/l)	Fe (μg/l)	Mn (μg/l)	Li (μg/l)	Zn (μg/l)	Cu (μg/l)
Carbonate hosted																											
Upper	(1)	41.3	7.7	27.3	4.8	11.2	−179	−20.3	−5.6	0.0	1200	132	711	24.3	6.2	0.05	37.0	258	43.5	6.3	4.9	1.7	35	6	40	16	4
Middle	(2)	22.0	7.2	27.1	−1.3	7.1	−160	−20.1	−6.5	0.0	1195	166	688	36.7	5.4	0.06	30.0	246	48.1	5.5	4.6	1.6	35	14	34	16	< 3
Cave	(3)	29.8	7.0	27.7	1.8	12.5	−160	−20.5	−8.5	1.6	1162	126	696	45.7	5.4	0.08	27.0	250	45.9	5.5	4.5	1.6	22	12	36	15	5
Basin	(4)	31.8	6.8	27.9	−2.1	13.7	−163	−20.2	−6.6	–	2026	154	1330	14.7	5.4	0.39	31.0	414	75.6	7.1	6.3	3.1	36	15	50	19	8
Mist Mountain	(5)	33.0	7.5	16.7	N/A	14.7	−151	−20.2	0.8	1.5	529	79.2	280	N/A	2.8	0.17	24.8	111	24.8	5.3	1.0	0.76	7	2	11	8	< 3
Radium	(6)	44.0	6.7	18.8	N/A	10.5	−154	−18.8	−5.9	2.9	828	217	356	N/A	13.2	< 1	38.6	150	33.2	14.9	3.3	1.6	31	12	40	24	7
Fairmont	(7)	46.7	6.3	17.9	N/A	13.0	−145	−18.8	−6.4	2.5	2277	685	929	N/A	34.0	< 1	32.9	451	107	29.0	5.5	3.5	27	38	44	69	12
Lussier Canyon	(8)	43.2	7.1	20.5	12.6	7.3	−145	−18.3	−7.0	0.8	2937	222	148	32.0	1400	0.52	36.6	115	24.8	979	10.6	1.1	23	8	80	16	6
Ram Creek	(9)	36.5	7.7	18.0	N/A	5.8	−141	−17.3	−9.0	4.8	294	148	56.0	N/A	1.2	< 1	21.3	49.2	14.5	2.4	1.3	0.16	< 5	4	2	5	< 3
Wildhorse River	(10)	31.0	7.1	20.3	N/A	17.5	−138	−18.7	−4.0	1.5	1629	105	1038	N/A	2.4	0.21	30.7	378	59.5	5.9	6.2	2.6	32	13	23	9	12
Fording Mt.	(11)	20.5	7.2	24.7	−11.8	–	−154	−19.9	−9.8	< 1	3051	269	1483	123	356	< 1	16.8	375	104	423	18.6	6.0	83	14	921	3	11
Wolfenden	(12)	27.7	6.8	9.6	N/A	–	−147	−19.1	–	–	1097	531	210	N/A	78.0	4.5	18.2	120	84.7	48.4	4.6	1.8	111	850	17	–	–
Toby Creek	(13)	8.9	6.3	30.4	N/A	11.4	−160	−19.0	−7.0	–	3068	1307	900	N/A	13.0	< 1	70.0	509	124	137	5.9	2.1	40	899	148	19	12
Albert Canyon	(14)	25.7	7.7	14.2	N/A	−0.8	−142	−18.9	−5.9	4.5	356	174	20.5	N/A	15.4	1.3	43.2	53.1	13.2	33.9	3.1	0.21	64	4	567	3	4
Miette	(15)	51.8	6.9	18.8	−5.0	–	−164	−20.4	−2.1	<	1828	127	1168	1.0	4.0	< 1	52.2	375	64.5	9.8	14.8	12.5	43	17	83	4	11
Cold Sulphur	(16)	8.8	7.0	27.5	5.7	4.1	−163	−20.0	−10.6	<	728	265	168	10.0	82.2	9.2	8.2	95.0	32.1	66.2	9.8	1.8	24	8	319	1	3
Liard	(17)	50.0	6.5	22.4	2.0	11.9	−179	−22.2	−4.8	1.0	1177	180	592	0.4	16.7	< 1	94.1	226	34.4	16.4	10.1	7.7	24	17	92	10	7
Takhini	(18)	46.2	6.6	15.2	N/A	15.6	−178	−22.2	−4.1	1.0	2619	112	1670	N/A	1.0	0.23	89.1	611	79.2	35.1	8.8	13.4	490	32	33	16	15
Atlin	(19)	28.8	7.1	−10.1	N/A	−4.2	−162	−21.4	−5.1	2.0	453	289	32.0	N/A	0.0	< 1	32.9	74.5	20.2	3.4	0.9	0.20	15	5	3	4	3
Silicate hosted																											
Dewar Creek	(20)	82.8	6.4	12.1	N/A	0.8	−149	−20.1	−4.9	<	878	149	287	0.1	54.0	0.04	139	27.9	0.3	206	10.9	3.3	42	58	907	6	4
Ainsworth	(21)	45.0	6.5	11.1	N/A	−2.4	−145	−18.5	−4.0	6.2	1739	1071	58.0	N/A	46.7	0.12	130	163	5.4	243	20.9	1.4	21	487	682	24	< 3
Halcyon	(22)	50.7	7.7	9.9	−12.9	2.6	−145	−19.2	4.4	0.8	752	46.0	396	12.2	5.7	< 1	77.7	57.4	0.6	159	6.9	2.5	24	11	643	33	0
Halfway	(23)	58.9	8.2	7.9	−0.8	8.0	−146	−18.4	−22.2	2.0	805	19.0	490	1.0	4.7	< 1	52.8	158	0.1	72.0	3.8	4.8	28	9	62	33	5
St. Leon	(24)	46.5	8.4	8.2	−8.0	7.6	−151	−19.7	−12.3	3.9	957	59.0	560	3.8	5.0	< 1	63.8	142	0.1	116	5.8	5.2	23	11	236	11	3
Nakusp	(25)	55.8	7.9	8.0	−5.8	7.3	−145	−18.9	–	0.5	599	80.0	290	5.2	1.5	< 1	62.0	68.7	0.3	85.5	5.8	4.7	21	8	71	30	< 3
KLO	(26)	22.7	6.4	6.6	N/A	7.0	−136	−17.8	−4.6	<	1358	815	45.5	N/A	3.8	< 1	122	196	26.6	141	6.4	1.7	2160	582	153	5	7
Lakelse	(27)	63.0	7.8	8.5	N/A	2.4	−129	−15.7	−11.6	2.5	1085	20.2	360	0.1	184	< 1	134	76.2	0.1	299	7.9	4.2	49	10	135	5	4
Hot Springs Cove	(28)	58.5	7.8	31.0	−1.0	10.4	−73	−10.4	−2.6	0.2	469	20.9	36.0	8.2	211	9.6	37.3	18.2	0.1	143	2.1	0.17	15	3	67	4	< 3
Flores Island	(29)	22.0	9.5	11.4	−5.6	5.6	−65	−9.4	−24.9	1.0	144	47.0	11.6	13.9	9.9	0.47	36.4	1.8	0.1	36.8	0.4	0.01	17	0	10	3	0
Volcanic																											
Harrison	(30)	62.4	7.7	12.9	N/A	4.0	−106	−14.1	−9.0	2.0	1379	19.6	547	N/A	287	< 1	68.9	89.2	0.1	355	11.7	1.3	16	9	164	3	5
Sloquet Creek	(31)	60.8	8.6	13.8	N/A	5.9	−120	−15.3	−8.4	4.0	727	25.8	375	N/A	59.7	< 1	65.2	83.5	0.0	114	3.1	0.50	10	9	24	2	6
St. Angus	(32)	50.0	7.9	8.7	N/A	3.5	−129	−16.6	−14.7	1.5	938	18.6	434	N/A	18.6	9.2	57.6	157	0.3	242	7.3	2.7	14	27	202	3	5
Meager Creek	(33)	47.0	7.2	5.8	N/A	−0.6	−123	−15.3	−5.0	4.0	1853	445	125	N/A	543	9.7	172	77.5	24.7	419	44.6	2.4	50	257	1150	3	5

precipitated from filtered water by the addition of $BaCl_2$. The water was then acidified to pH < 2 in order to dissolve any $BaCO_3$. If HS^- was not present, SO_4 was precipitated in the field. For $\delta^{13}C$ in bicarbonate, HCO_3 was precipitated by the addition of a saturated solution of ammoniacal $SrCl_2$ chloride in an evacuated CO_2 free container. The $SrCO_3$ precipitate was filtered, washed with hot water, and dried, in a N_2 atmosphere.

Chemical and stable isotope analyses were conducted at the University of Calgary. Alkalinity was determined using an Orion 960 auto-titrator within 7 days of sample collection. Anions were measured by ion liquid chromatography and cation concentrations were measured by flame atomic absorption. Analytical error in concentration measurements was estimated to be less than 2%.

Stable isotope compositions ($^{18}O/^{16}O$, D/H, $^{34}S/^{32}S$, $^{13}C/^{12}C$) are expressed using the usual δ notation:

$$\delta(‰) = [(R_{sample} - R_{standard})/(R_{standard})] \times 10^3,$$

where R is the ratio of the heavy to light isotope abundances. The standards used are V-SMOW for O and H, V-CDT for S, and V-PDB for C. For $\delta^{34}S$ analyses, SO_2 was prepared using the methods of Yanagisawa and Sakai (1983), $\delta^{18}O_{(SO_4)}$ was measured with CO_2 prepared by graphite reduction of $BaSO_4$ (Shakur, 1982), $\delta^{18}O_{(H_2O)}$ was measured on CO_2 isotopically equilibrated with H_2O (Epstein and Mayeda, 1953), and δD was measured using H_2 produced by the Zn-reduction method of Coleman et al. (1982). $\delta^{13}C_{(HCO_3)}$ was measured on CO_2 released by reacting $SrCO_3$ with phosphoric acid, following the method of McCrea (1950). Combined sampling and analytical errors for isotope data were estimated to be $\pm$0.2‰ for $\delta^{18}O_{(H_2O)}$ and $\delta^{34}S$, $\pm$1‰ for δD and $\delta^{18}O_{(SO_4)}$ and $\pm$0.3‰ for $\delta^{13}C$.

4. Geochemistry of thermal springs

Although the existence of thermal springs in Canada has been known since the late 19th century, few have been studied in any detail. Most work has focused on springs in National Parks (e.g. van Everdingen, 1972; 1984; Krouse, 1976; Mazor et al., 1983) largely due to their fame, and springs in the Garibaldi volcanic belt due to the potential for geothermal energy production (e.g. Souther, 1976; Clark et al., 1982; Ghomshei and Clark, 1993). Other than focused studies, chemical analyses of thermal springs are only rarely available as footnotes in reports of the Geological Survey of Canada. When comparing available analyses, the one noticeable feature is that the temperature and chemistry of individual thermal springs are constant

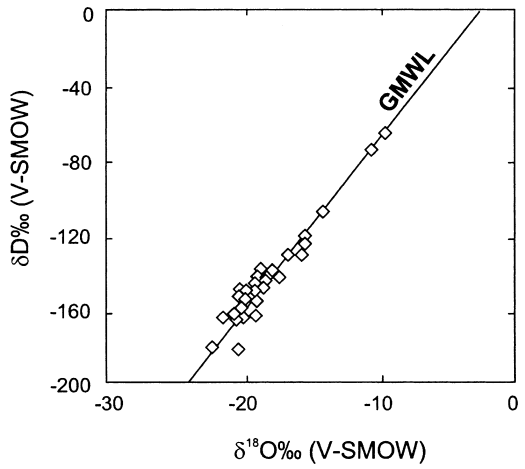

Fig. 2. δD vs. $\delta^{18}O$ for thermal spring waters. Springs tend to plot along the global meteoric water line (GMWL) indicating a meteoric origin of the thermal waters.

through time (see examples in Table 1). This consistency indicates that thermal systems develop chemical compositions in equilibrium (perhaps metastable) with the host rock, and/or are controlled by steady state kinetic processes between the fluids and the host rock. Biological processes likely also play a role in controlling the chemistry of thermal springs, particularly the concentrations of S and C aqueous species, given the common occurrence of SO_4 reducing bacteria in spring water (e.g. Smejkal et al., 1971; Krouse, 1976). Here the water–rock interaction and biological influences of the chemistry of thermal springs are examined. However, it is important to first identify the source of the water itself.

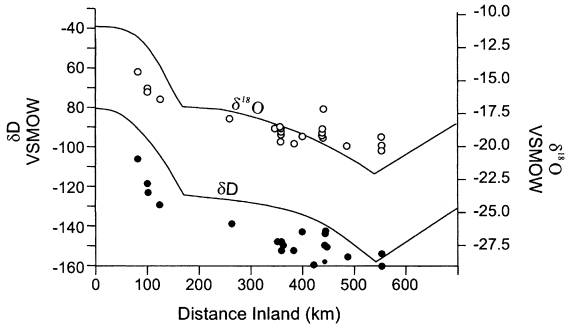

Fig. 3. Inland variation in the δD and $\delta^{18}O$ values of meteoric water (solid lines, after Yonge et al., 1989) with values of δD (filled circles) and $\delta^{18}O$ (open circles) for thermal springs superimposed. Distance is measured perpendicular to the NW–SE trending west coast of British Columbia (profile line A–A′ in Fig. 1). Only springs along A–A′ are plotted. δD values of thermal springs decrease inland, consistent with the continental effect of Dansgaard (1964).

4.1. $\delta^{18}O$ and δD: The source of water

The $\delta^{18}O$ and δD values for the thermal springs sampled (Table 2) are plotted in Fig. 2. Most of the waters lie on, with a few samples to the right of, the global meteoric water line. This indicates that the thermal waters have a meteoric origin, consistent with other studies that demonstrate a meteoric origin for waters from thermal springs around the world (e.g. Craig, 1963; Michelot et al., 1993; Sturchio et al., 1996; Wang and Shpeyzer, 1997). In Fig. 3 the δD and $\delta^{18}O$ values of spring waters in the southern Cordillera, along profile A–A′ in Fig. 1, show a trend that decreases inland (δD from −100 to −160‰). This is consistent with the continental effect of Dansgaard (1964), which predicts an inland depletion in the heavy isotopes of precipitation. For comparison, a profile of the inland variation of δD and $\delta^{18}O$ for surface water across the southern Cordillera (Yonge et al., 1989) is plotted as the curves in Fig. 3. The δD values of thermal springs follow a similar trend as surface waters from Yonge et al. (1989), but plot consistently below the profile. The $\delta^{18}O$ values also show a similar trend, however, they are generally more positive than surface waters in the eastern Cordillera. The profile of Yonge et al. (1989) is based on samples of small tributaries. Thus it averages variations in the stable isotope composition of meteoric water related to orographic effects and seasonal temperature variations. Thus a possible explanation of the more negative values of δD of springs may be either a function of recharge areas being at higher elevations and/or recharge being dominated by spring snow melt. Alternatively, if the spring systems have a long enough transit time, the more negative values of δD could represent recharge during a period of colder climate. The high $\delta^{18}O$ values of springs compared to surface waters in the eastern part of the profile is likely a function of more rapid exchange of ^{18}O with carbonate rocks that dominate the eastern Cordillera.

The above data indicate that thermal spring waters have a meteoric origin, and therefore must be heated by deep circulation.

4.2. Controls on the major ion chemistry of thermal springs

Following Souther (1992), springs are divided by geological association into 3 groups: (1) carbonate-hosted springs, (2) silicate-hosted springs (igneous and metamorphic rock in nonvolcanic regions) and (3) springs hosted in Quaternary volcanic belts. The thermal springs sampled (Table 2) show a range of TDS from 144 to 3068 mg/l. In general, carbonate-hosted springs have the highest TDS and lowest SiO_2, whereas silicate and volcanic-hosted springs have low TDS and low to high SiO_2 (Fig. 4). Silicate-hosted springs show a reasonable linear correlation between TDS and SiO_2, as would be expected for waters in contact with silicate rock. The Piper diagram in Fig. 5 illustrates that thermal springs vary from Ca–Mg rich to Na–K rich waters, largely as a function of host rock. Carbonate-hosted springs have a $Ca–HCO_3–SO_4$ chemistry, with the exception of the Lussier Canyon spring (No. 8), which is Na–Cl rich (possibly indicating dissolution of halite). Silicate and volcanic hosted springs tend to be Na rich and show a wide range of anion compositions.

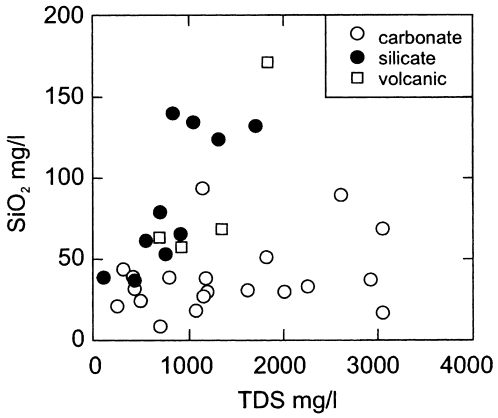

Fig. 4. Plot of total dissolved solids (TDS) versus SiO_2. Silicate hosted springs show a reasonable correlation between TDS and SiO_2.

Although the chemical make up of the different springs is highly variable, Table 1 illustrates that the chemistry of any particular spring is constant through time. As stated above, this suggests that either equilibrium and/or steady state processes are controlling the spring chemistry. Although theoretically possible, it is inherently difficult to test if a steady state process is controlling the chemistry of thermal springs, particularly without knowing details of the flow path. For this paper the authors evaluate equilibrium processes controlling spring chemistry based on a thermodynamic model of water–rock interaction.

Because water–rock interaction is largely dependant on pH and temperature, it is necessary to first define these values at some point in the system. The pH and temperature measured at the surface outlet of springs are unlikely to represent equilibrium conditions due to near-surface cooling, and evolution of CO_2. Therefore, it is necessary to calculate the pH and temperature in the subsurface. Determining pH at subsurface conditions is difficult without being able to quantify CO_2 loss from the system. Given that carbonate minerals are present in most rock types, as either a primary mineral or an alteration product (particularly in hydrothermal systems), the pH in the subsurface is calcu-

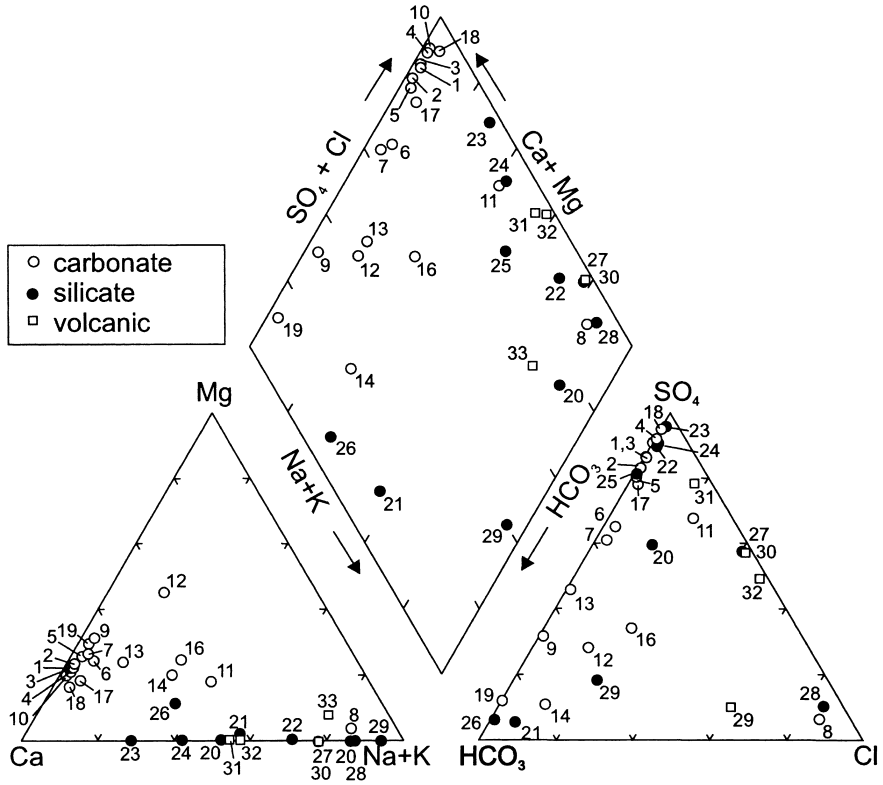

Fig. 5. Piper diagram, in meq/l, for thermal springs in this study. Numbers refer to springs in Table 2. Springs vary from Ca–Mg rich to Na–K rich largely as a function of host rock.

lated from the Ca^{2+} and HCO_3^- content and the equilibrium constant, assuming waters are in equilibrium with calcite.

Only direct physical measurement can provide reliable subsurface temperatures. Since wells were not available for direct measurement, aqueous geothermometers were used for each rocktype grouping. Results from the various geothermometers are presented in Table 3. In nonquartzose rocks, the solubility of Si at temperatures below 180°C is controlled by amorphous silica and/or chalcedony (Kharaka and Mariner, 1988), making the quartz geothermometer unreliable for carbonate hosted springs. The amorphous silica geothermometer consistently gives temperatures below those measured at the surface, suggesting that the solubility of Si in carbonate hosted springs is controlled by a more stable phase like chalcedony. At temperatures less than 180°C, high amounts of Ca can affect the accuracy of the Na/K geothermometer (Kharaka and Mariner, 1988). This is evident by the extraordinarily high Na/K temperatures calculated for carbonate-hosted springs in the Rocky Mountains. The Na–K–Ca geothermometer of Fournier and Truesdell (1973) accounts for the effect of high Ca. However, Ca loss through calcite precipitation may also affect Na–K–Ca temperatures. Carbonate-hosted springs commonly have associated tufa deposits, indicating that Ca is lost from the system, and that the Na–K–Ca temperatures are unreliable. The Mg corrected Na–K–Ca geothermometer gives values less than 0°C and thus does not work in these systems. The Mg/Li geothermometer tends to give temperatures lower than those measured at the surface in carbonate-hosted springs. Temperatures derived from the O isotope values of SO_4 and H_2O (Mizutani and Rafter, 1969) also tend to be below those measured at the surface. The temperatures in most thermal springs in the study area are likely too low for equilibrium exchange of O isotopes between SO_4–H_2O to occur rapidly enough at the pH of the springs (Chiba and Sakai, 1985). Therefore, for carbonate hosted springs we have accepted temperatures from the chalcedony geothermometer have been accepted.

In silicate and volcanic hosted springs, the amorphous silica geothermometer again gives values lower than surface temperatures, suggesting Si is controlled by quartz or chalcedony. Most of the temperatures for quartz and chalcedony fall in the range between 90 to

Table 3
Temperatures calculated by geothermometry. (–) = temperatures calculated below 0°C, *T*max = temperature selected from geothermometers (see text for details)

Spring	No.	$T_{measured}$ (°C)	amph. Si (°C)	Quartz (°C)	Chal. (°C)	Na/K (°C)	Na–K–Ca (°C)	Mg–Ca–Na–K (°C)	Mg/Li (°C)	SO_4–H_2O (°C)	*T*max (°C)	pH (measured)	pH (calculated)
Carbonate hosted													
Upper	(1)	41	–	97	67	490	211	–	13	25	67	7.7	7.3
Middle	(2)	22	–	88	57	506	213	–	10	44	57	7.2	7.2
Cave	(3)	30	–	83	52	500	211	–	11	19	52	7.0	7.5
Basin	(4)	32	–	90	59	522	217	–	12	16	59	6.8	7.0
Mist Mountain	(5)	33	–	80	48	281	142	–	–	12	48	7.5	7.6
Radium	(6)	44	–	99	69	295	162	–	15	34	69	6.7	7.1
Fairmont	(7)	47	–	92	62	279	157	–	7	24	62	6.3	6.3
Lussier Canyon	(8)	43	–	97	67	80	95	–	30	53	67	7.1	7.4
Ram Creek	(9)	37	–	73	42	420	186	–	–	66	42	7.7	7.6
Wildhorse River	(10)	31	–	89	58	559	224	–	2	8	58	7.1	7.1
Fording Mountain	(11)	21	–	65	33	155	132	–	65	–	33	7.2	7.2
Wolfenden	(12)	28	–	68	36	213	142	–	–	94	36	6.8	6.8
Toby Creek	(13)	9	10	129	102	154	113	–	26	30	102	6.3	6.0
Albert Canyon	(14)	26	–	104	74	210	142	–	77	101	74	7.7	7.5
Miette	(15)	52	–	114	85	661	262	–	22	–	85	6.9	7.1
Cold Sulphur	(16)	9	–	39	6	253	171	–	54	61	39	7.0	7.2
Liard	(17)	50	24	145	120	446	218	–	29	15	120	6.5	7.1
Takhini	(18)	46	22	143	116	311	171	–	5	2	116	6.6	7.0
Atlin	(19)	29	–	92	61	314	151	–	999	109	61	7.1	7.1
Silicate hosted													
Dewar Creek	(20)	83	46	169	147	168	149	–	144	81	147	6.4	8.0
Ainsworth	(21)	45	42	165	142	204	161	–	93	119	163	6.5	6.4
Halcyon	(22)	51	–	134	107	155	131	–	123	75	132	7.7	8.6
Halfway	(23)	59	–	113	84	168	121	121	81	49	117	8.2	8.3
St.Leon	(24)	47	3	121	93	164	126	126	165	44	123	8.4	7.8
Nakusp	(25)	56	3	122	93	185	140	–	382	49	131	7.9	7.9
KLO	(26)	23	39	161	137	157	122	–	41	57	137	6.4	6.4
Lakelse	(27)	63	43	166	143	125	117	–	107	101	141	7.8	9.1
Hot Springs Cove	(28)	59	–	97	67	93	94	–	85	81	95	7.8	9.4
Flores Island	(29)	22	–	78	46	75	78	–	49	129	78	9.5	11.2
Volcanic													
Harrison	(30)	62	8	127	100	137	127	127	113	101	127	7.7	8.6
Sloquet Creek	(31)	61	3	121	93	126	105	105	84	78	116	8.6	8.4
St. Angus	(32)	50	–	118	89	132	115	115	102	86	116	7.9	8.2
Meager	(33)	47	60	184	163	222	188	–	87	132	186	7.2	7.1

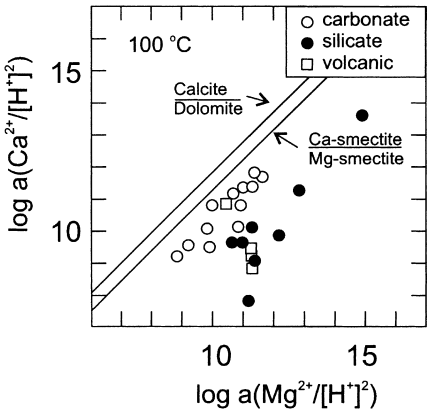

Fig. 6. Plot of log a($Ca^{2+}/[H^+]^2$) versus log a($Mg^{2+}/[H^+]^2$). Thermal springs define a strong trend with a slope of 1. The two phase boundaries with a slope of 1 in the range of activity ratios for the springs are also plotted (calculated at 300 bar and 100°C).

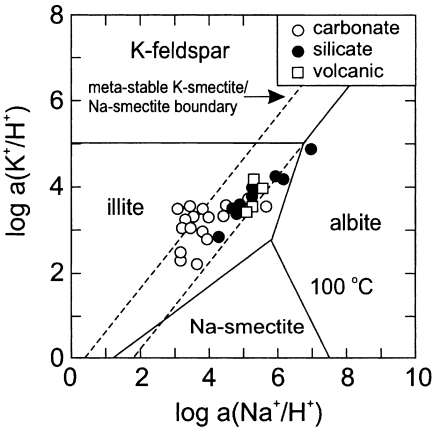

Fig. 7. Plot of log a(Na^+/H^+) versus log a(K^+/H^+) illustrating possible reaction boundaries that may control water composition. The scatter of carbonate springs is likely related to the lack of Na–K minerals in the host rock. Boundaries, stable (solid lines) and meta-stable (dashed lines), are calculated at 300 bar and 100°C.

180°C, where it is not possible to tell without independent data which phase controls silica activity (Arnorsson, 1975). Quartz temperatures tend to be fairly consistent with the Na–K–Ca geothermometer, which is favored over Na–K due to more rapid equilibration (Kacandes and Grandstaff, 1989). Therefore, for silicate and volcanic hosted springs, an average of quartz and Na–K–Ca temperatures is used (T_{max} in Table 3).

The subsurface values for pH and temperature estimated above were used for chemical speciation and activity calculations for subsurface conditions using the geochemical modeling package SOLMINEQ.88 PC/SHELL (Wiwchar et al., 1988). $Ca^{2+}/(H^+)^2$ and $Mg^{2+}/(H^+)^2$ activity ratios determined from the water compositions using SOLMINEQ.88, at subsurface temperature and pH, are plotted in Fig. 6. Activity data for carbonate-hosted springs define a strong trend with a slope of 1 ($r^2 = 0.83$). Activity data for silicate-hosted springs plot along a similar trend that is offset from the carbonate springs. In volcanic-hosted springs, activity data do not show a discernable trend, however they plot in the same range of values as the other springs. A slope of 1 in a Ca–Mg activity plot suggests a 1:1 Ca–Mg exchange reaction is controlling the ion ratios. In order to identify potential exchange reactions, mineral stability boundaries were calculated at 100°C using the program PTA (Brown et al., 1988) for the system Ca, Mg, Al, Si, C, O and H. PTA was modified by the addition of thermodynamic data for beidellite (after Abercrombie, 1988). The range of possible reactions was restricted by only considering common rock forming Ca and Mg minerals (Table 4). Of the over 7000 stable and meta-stable reactions considered, only 2 have a 1:1 Ca–Mg exchange boundary in the range of activities calculated for thermal springs:

$$20\text{Mg-beidellite} + 3Ca^{2+} = 3Mg^{2+} + 20\text{Ca-beidellite} \quad (1)$$

$$2\text{calcite} + Mg^{2+} = \text{dolomite} + Ca^{2+}, \quad (2)$$

where Ca– and Mg–beidellite are pure endmembers of smectite with unit activity. This suggests that equilibrium reactions with minerals in reactions (1) and (2) may be controlling the Ca/Mg ratio in the various springs. This is feasible, considering that smectite is one of the most ubiquitous minerals in geological settings; smectite is present as detrital particles in sedimentary rocks, and is a common alteration product of igneous and metamorphic minerals. Likewise, carbonate minerals are present in most rock types as either a primary mineral or an alteration product, particularly in hydrothermal systems. The phase boundaries for the pure endmember minerals (unit activity) are plotted as lines on Fig. 6. Also plotted are the $Ca^{2+}/(H^+)^2$ and $Mg^{2+}/(H^+)^2$ activity ratios determined from water analysis of individual springs. The data trend, with a slope of 1, is consistent with equilibrium exchange con-

Table 4
Common rock forming minerals used for phase boundary calculations

plagioclase	illite	quartz
K-feldspar	kaolinite	chalcedony
Ca-smectite	Na-smectite	K-smectite
Mg-smectite	calcite	dolomite
heulandite	laumonite	

trolling the water chemistry. The observation that activity data from the thermal springs in this study do not lie directly on the phase boundaries suggests that the minerals involved in these reactions are not pure endmember components (variation in the Ca–Mg ratio of smectite will move the location of the phase boundary, however the slope will remain the same).

Na^+/H^+ and K^+/H^+ activity ratios determined from the water compositions using SOLMINEQ.88, at estimated subsurface temperature and pH, are plotted in Fig. 7. Activity data for silicate-hosted springs define a slope of 1, suggesting a 1:1 Na–K exchange reaction is controlling the ion ratios. In contrast, activity data for carbonate and volcanic-hosted springs do not define any trend. Mineral stability boundaries were calculated at 100°C for the system Na, K, Al, Si, O and H, for minerals in Table 4. Results indicate that only 2 reactions have a 1:1 Na–K exchange boundary in the range of activities calculated for thermal springs:

$$10\text{K-beidellite} + 3Na^+ = 3K^+ + 10\text{Na-beidellite} \quad (3)$$

$$\text{K-feldspar} + Na^+ = \text{Albite} + K^+. \quad (4)$$

The phase boundaries for the pure endmember minerals (unit activity) are plotted as lines on Fig. 7. Also plotted are the Na^+/H^+ and K^+/H^+ activity ratios determined from water analysis of individual springs. Na^+/H^+ and K^+/H^+ ratios for silicate and volcanic hosted springs lie on the meta-stable extension of the K-feldspar/albite reaction boundary, suggesting that this reaction is controlling the Na/K activity ratio for these springs, and that illite and smectite, if present in silicate rocks, have no effect on the water composition. Activity data for carbonate-hosted springs plot within the illite stability field, and in between the meta-stable boundaries for the K-feldspar/albite reaction and Na, K-smectite exchange. The scatter of carbonate springs is likely related to the lack of Na-K minerals in carbonate rock.

The above demonstrates how equilibrium exchange reactions with common rock forming minerals may control the activity ratios of the major cations in thermal spring waters. These results are consistent with Kacandes and Grandstaff (1989) who show that in numerous geothermal fields, and in experimental water–rock interaction studies, that the Na/K and Ca/Mg ratios tend to be consistent and define 1:1 slopes. They suggest that ion-exchange reactions may best explain the consistency in the ion ratios.

5. The sulfur cycle

As stated in the introduction, many hydrothermal ore models rely on reduced S being introduced at depth by the deep circulation of meteoric water. Here the processes in active thermal springs that affect the S cycle are examined. Both SO_4 and sulfide occur in thermal springs, with SO_4 being the dominant form. Concentrations are highly variable in the springs examined (11–1670 mg/l SO_4, 0–123 mg/l H_2S). Although present in precipitation, SO_4 concentrations are too low (< 5 mg/l) to be the source of S in thermal springs. Thus, SO_4 must be derived from rock weathering; either oxidation of sulfide minerals or dissolution of evaporite minerals (gypsum and anhydrite). The sources of SO_4 and HS^- in thermal springs are examined below.

5.1. The origin of sulfate

Figure 8 plots the $\delta^{34}S_{SO_4}$ versus SO_4 concentration. Note that carbonate hosted springs tend to have both higher $\delta^{34}S_{SO_4}$ values (> 15‰) and higher SO_4 concentrations compared to silicate and volcanic hosted springs. Figure 9 shows the $\delta^{34}S$ values of SO_4, sulfide (when present), and the weighted average $\delta^{34}S$ for SO_4 and sulfide where applicable. Grasby and Hutcheon (1999) demonstrate that distribution of thermal springs in the Cordillera is related to major and/or anomalous structural features. Figure 9 shows that the Sulphur Mountain Thrust (SMT) and Redwall Fault (RWF) have a number of associated springs that have similar values for $\delta^{34}S_{SO_4}$. The similarity in $\delta^{34}S_{SO_4}$ from springs associated with the same fault and rock type, suggests that, as in Van Everdingen et al. (1982), the $\delta^{34}S_{SO_4}$ values are representative of the S source and are not drastically altered by biological activity. Therefore, the $\delta^{34}S_{SO_4}$ values can be used to indicate the source of S in thermal springs. In carbonate hosted springs, SO_4 may be derived from dissolution of SO_4

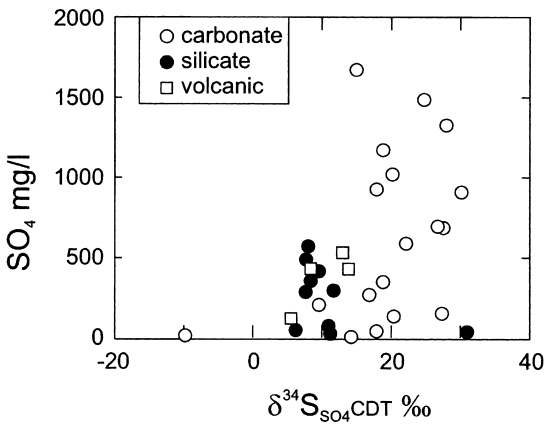

Fig. 8. $\delta^{34}S$ versus SO_4 concentration. Carbonate hosted springs tend to have high SO_4 concentrations with $\delta^{34}S$ values consistent with dissolution of evaporite minerals.

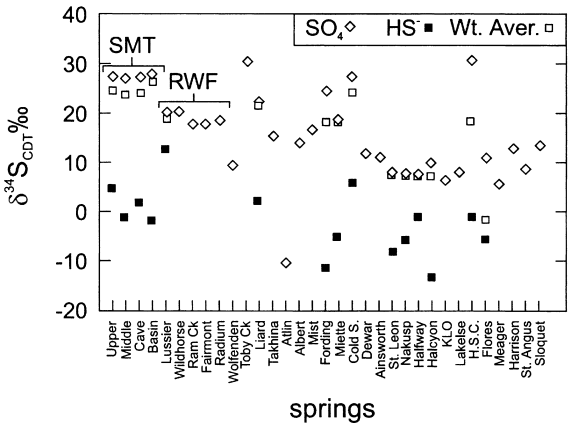

Fig. 9. Plot of $\delta^{34}S$ for dissolved SO_4, and HS^- for springs in this study. The weighted average $\delta^{34}S$ is shown where applicable. Springs associated with the Sulphur Mountain Thrust (SMT) and Redwall Fault (RWF) are indicated (see text).

minerals (primarily gypsum and anhydrite) or oxidation of pyrite (secondary SO_4). The range of $\delta^{34}S_{SO_4}$ values in carbonate hosted springs (+15 to +30‰) is consistent with the range observed in Palaeozoic evaporites (Claypool et al., 1980), and significantly higher than the range for sulfide minerals (Krouse, 1980), indicating that SO_4 is derived from dissolution of evaporites. Although SO_4 is likely derived from evaporite dissolution, SOLMINEQ.88 indicates that most springs are undersaturated with respect to gypsum and anhydrite. This suggests that the concentration of SO_4 in these springs may be controlled by a steady state dissolution process, that is perhaps influenced by biological SO_4 reduction (McCready and Krouse, 1980). The influence of biological activity on the S cycle in thermal springs is discussed latter.

The $\delta^{34}S_{SO_4}$ values of silicate and volcanic hosted springs are higher than the terrestrial average (0 to +10‰), however they are still within the range observed for pyrite in igneous rocks (Krouse, 1980). One silicate-hosted spring, Sharp Point, has a much higher $\delta^{34}S_{SO_4}$ (+31‰). However, considering that this spring occurs only a few metres from the ocean, the weighted average value of SO_4 and H_2S, +18‰, is consistent with a signature of modern sea water SO_4 (+20‰) (Krouse, 1976; Phillips, 1994).

5.2. The origin of Sulfide

The origin of H_2S in thermal springs has been examined previously by Krouse et al. (1970) and Smejkal et al. (1971). They showed that in several springs in western Canada, large fractionations ($\Delta^{34}S_{SO_4\text{-}H_2S}$ up to 30‰) are related to reduction of SO_4 by two species of anaerobic bacteria. In addition, *Desulfotomaculum* (a strict anaerobe) was found, which like *Desulfovibrio* reduces SO_4^{2-} to HS^-. Figure 9 illustrates that, where present, the $\delta^{34}S$ of H_2S in spring water is always low relative to SO_4, consistent with Krouse et al. (1970). This, and evidence of biological cycling of SO_4 (discussed below), indicates that H_2S is largely derived from bacterial SO_4 reduction (BSR). This is consistent with the geothermometers discussed above that give temperatures below 140°C for most springs. Worden et al. (1995) indicate that temperatures on the order of 140°C are needed for thermochemical SO_4 reduction, even at geological time scales associated with petroleum formation.

5.3. Biological cycling of dissolved sulfate

A plot of $\delta^{18}O_{SO_4}$ versus $\delta^{18}O_{H_2O}$ (Fig. 10) shows that springs plot above the theoretical sulfide oxidation field of van Stempvoort and Krouse (1994) and below the average $\delta^{18}O_{SO_4}$ value for evaporites (+15‰; Claypool et al., 1980). Also, $\delta^{18}O_{SO_4}$ is generally positive and highly variable (over 25‰), whereas $\delta^{18}O_{H_2O}$ is negative and has only a 10‰ range. Three possible factors that may cause the relatively large variation observed in $\delta^{18}O_{SO_4}$ are: (1) equilibrium exchange of ^{18}O between SO_4 and water, (2) mixing of SO_4 derived from sulfide oxidation with SO_4 derived from dissolved evaporite minerals, and (3) biological cycling. The first two are less likely than the third for the following reasons. As discussed above, equilibrium isotope exchange reactions are too slow to be a significant control on $\delta^{18}O_{SO_4}$ at the temperatures and pH of the majority of thermal springs in this study, although,

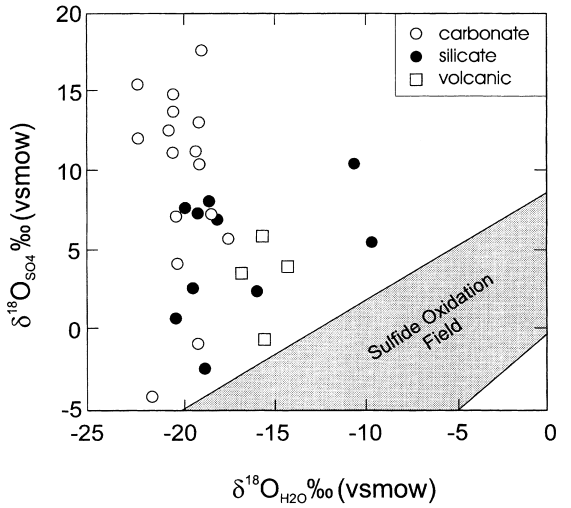

Fig. 10. Plot of $\delta^{18}O_{SO_4}$ versus $\delta^{18}O_{H_2O}$. The sulfide oxidation field of van Stempvoort and Krouse (1994) indicates the zone where oxidized sulfides are expected to plot.

equilibrium exchange may be possible in the higher temperature springs. If the $\delta^{18}O_{SO_4}$ is controlled by the oxidation of sulfide, springs would be expected to plot in the theoretical sulfide oxidation field of van Stempvoort and Krouse (1994) (Fig. 10). One possible method of obtaining $\delta^{18}O_{SO_4}$ values that are above the sulfide oxidation field, and below the average $\delta^{18}O_{SO_4}$ for evaporite minerals (+15‰, Claypool et al., 1980), is mixing of SO_4 from evaporites and SO_4 from sulfide oxidation. However, if the variability of the $\delta^{18}O$ composition of O in SO_4 was due to mixing of evaporite SO_4 with oxidized sulfide, the $\delta^{34}S$ value of SO_4 would be expected to decrease as $\delta^{18}O$ decreases. Figure 11 illustrates that carbonate-hosted springs related to the same fault (as in Fig. 9) have constant $\delta^{34}S_{SO_4}$ while $\delta^{18}O_{SO_4}$ is variable. If it is assumed that springs related to the same fault, and flowing through the same age rocks, derive their SO_4 from the same source (explaining the consistency in $\delta^{34}S_{SO_4}$) then some process must be causing variation in $\delta^{18}O_{SO_4}$ without affecting the $\delta^{34}S_{SO_4}$. One possible process is bacterial SO_4 reduction in a nearly closed system (i.e. there is no significant loss of reduced S from the system), followed by reoxidation.

Bacterial reduction and reoxidation of SO_4 was proposed by van Everdingen et al. (1982) to explain the variability of $\delta^{18}O_{SO_4}$ in the low temperature Page Springs of the Northwest Territories. They argue that if there is minimal escape of H_2S when SO_4 is reduced, the $\delta^{34}S$ composition of total S in the system will not be altered by biological cycling. However, biological cycling of S can have significant affects on the $\delta^{18}O$ composition of SO_4. For springs where dissolution of

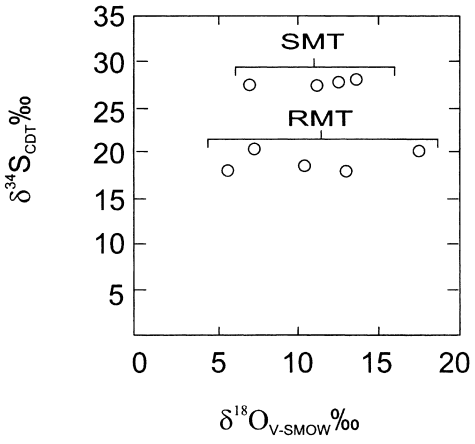

Fig. 11. Plot of $\delta^{34}S_{SO_4}$ versus $\delta^{18}O_{SO_4}$ for carbonate hosted springs associated with the Sulphur Mountain Thrust (SMT) and Redwall Fault (RWF). The small variation in $\delta^{34}S_{SO_4}$ compared to $\delta^{18}O_{SO_4}$ suggests that S cycling takes place with minimal loss of HS^- from the system.

SO_4 minerals is the dominant source of S, the $\delta^{18}O_{SO_4}$ should vary between +10 to 18‰ (Claypool et al., 1980). If the water becomes anoxic, then bacterial activity will reduce some portion of the SO_4 in the system, producing HS^-. As the waters ascend towards the surface they can be reoxidized, and HS^- will rapidly convert back to SO_4. During oxidation it is estimated that 60 to 100% of O_2 is derived from water, and the rest from air (Lloyd, 1967; van Stempvoort and Krouse, 1994). Thus the reoxidized SO_4 will be depleted in ^{18}O compared to the original SO_4. It follows then, that the more biological cycling of primary SO_4 that occurs, the more depleted the $\delta^{18}O$ of total SO_4 in the spring becomes. Thus the $\delta^{18}O_{SO_4}$ can provide a measure of the total amount of SO_4 that has been reduced in the system prior to HS^- being reoxidized. Based on this concept, van Everdingen et al. (1982) suggested that up to 30% of the SO_4 in the Page Springs has been reduced and reoxidized.

For the springs in Fig. 11, the small variation of $\delta^{34}S$, compared to $\delta^{18}O$ in SO_4 suggests that variable degrees of SO_4 reduction and reoxidation take place with minimal loss of HS^- from the system. Given that the $\delta^{34}S$ values for carbonate-hosted springs are consistent with derivation from evaporite minerals (see above), and that the $\delta^{18}O_{SO_4}$ values of evaporite minerals in the Phanerozoic are fairly well constrained (Claypool et al., 1980), it is possible to calculate the degree of bacterial cycling of SO_4 in a system where SO_4 is derived from evaporite dissolution.

The isotope composition of O in reoxidised SO_4 ($\delta^{18}O_{OX}$) will be the sum of the relative contributions of O from water ($\delta^{18}O_{H_2O}$) and atmospheric O_2 ($\delta^{18}O_{O_2}$), as defined by the general relation:

$$\delta^{18}O_{OX} = y(\delta^{18}O_{H_2O} + \varepsilon_{H_2O}) + (1 - y)(\delta^{18}O_{O_2} + \varepsilon_{O_2}) \quad (5)$$

where y is the fraction of O derived from water, and ε is a kinetic fractionation factor. The abiotic oxidation of sulfide to SO_4 goes through many intermediate steps making ε_{H_2O} difficult to determine. However, due to the rapid exchange of O between SO_3^{2-} and H_2O at the pH conditions of the thermal springs studied, ε_{H_2O} would be minimal (van Stempvoort and Krouse, 1994). For microbial oxidation, SO_3^{2-} is oxidized by an enzyme-catalyzed reaction that derives O from ambient water (Kelly, 1982). Thus biotic oxidation should have close to a 100% contribution of O from H_2O.

The cycling of primary SO_4 may be calculated using an isotope balance approach, where the % biological cycling of SO_4 (i.e. the proportion of SO_4 in the spring water that has been reduced and then reoxidized = X%) is defined as:

$$X\% = \frac{\delta^{18}O_{SPR} - \delta^{18}O_{EVAP}}{\delta^{18}O_{OX} - \delta^{18}O_{EVAP}} \times 100\% \quad (6)$$

Table 5
Calculated % biological cycling of SO_4 in carbonate hosted thermal springs. Negative results are listed as 0

Location	No.	60% H_2O	100% H_2O	60% H_2O			100% H_2O			Average
				12‰	15‰	17‰	12‰	15‰	17‰	
Upper	1	18	11	6	21	29	3	11	16	14.22
Middle	2	37	22	33	45	50	15	22	27	32.1166
Cave	3	12	7	−3	14	23	−1	7	12	8.55498
Basin	4	6	4	−11	7	17	−5	4	9	3.41772
Mist Mountain	5	1	1	−18	2	12	−8	1	6	−1.1446
Radium	6	22	13	11	27	35	5	13	18	18.223
Fairmont	7	10	6	−7	12	21	−3	6	11	6.63972
Lussier Canyon	8	39	23	35	46	52	15	23	27	33.1835
Ram Creek	9	47	28	48	57	62	21	28	33	41.5819
Wildhorse River	10	0	0	−40	−15	−3	−18	−7	−1	−14.07
Toby Creek	13	18	11	4	21	30	2	11	16	13.9266
Albert Canyon	14	77	47	92	93	94	41	47	50	69.4434
Cold Sulphur	16	51	31	54	62	66	25	31	35	45.3245
Liard	17	14	8	0	16	24	0	8	13	10.391
Takhini	18	0	0	−22	−3	7	−10	−2	4	−4.4499
Atlin	19	87	53	105	104	104	49	53	55	78.211

where $\delta^{18}O_{SPR}$ is the $\delta^{18}O_{SO_4}$ measured in the spring, and $\delta^{18}O_{EVAP}$ is the average value for evaporite minerals (+15‰). If exposure to atmospheric O_2 is minimal, or if microbial oxidation is prominent, then the majority of O in the reoxidised SO_4 will be from water. However, if abiotic oxidation occurs in conjunction with exposure to atmospheric O_2, then up to 40% of O in the reoxidised SO_4 could be from atmospheric O_2. The % biological cycling was calculated for the two extremes (60 and 100% O_2 from H_2O), where $\delta^{18}O_{OX}$ is from Eq. (5), and represents the calculated net value for O involved in the oxidation of reduced S, where $\varepsilon_{H_2O}=0$, and $\varepsilon_{O_2}=-8.7‰$ (Lloyd, 1967), $y = 0.6$ and 1, and the $\delta^{18}O_{O_2}$ used is +23‰. To avoid the possible effects of equilibrium exchange of ^{18}O, biological cycling of S in thermal springs is calculated only for springs with temperatures calculated by geothermometry that are $<100^{\circ}C$. Only springs that are hosted by carbonate rocks, and with $\delta^{34}S$ values consistent with derivation from evaporites, are considered.

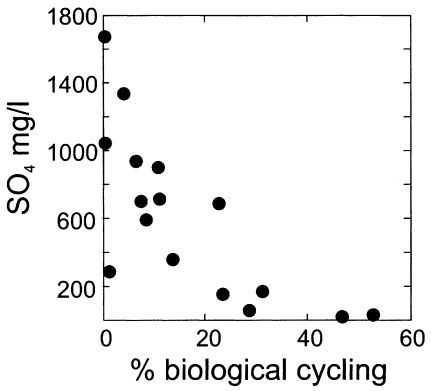

Fig. 12. Calculated % of biological cycling for carbonate hosted springs versus measured SO_4 concentration. The inverse relationship indicates that SO_4 is not a limiting nutrient.

For the case of 60% contribution from H_2O, calculated values for biological cycling vary from 0 to 87% (Table 5). Values are 2/3 that if all the O is derived from H_2O (i.e. up to 53% biological cycling). These are the most realistic values given the potential for microbial oxidation of S and the limited contact of subsurface water with the atmosphere. As well, the fO_2 should be low due to buffering by magnetite–hematite or similar redox couples at the temperatures of the springs considered (Kacandes and Grandstaff, 1989). The values calculated are also a function of the values for ε chosen. Although this would affect the actual % cycling calculated, the relative difference would not be affected, allowing a comparison of different springs. Figure 12 illustrates that the calculated amount of biological cycling of S varies inversely with SO_4 concentration. The results of these calculations indicate that although an essential source of O, SO_4 is not a limiting nutrient for biological activity in the thermal systems we examined.

6. The carbon cycle

For biologically mediated SO_4 reduction, a represen-

tative reaction may be written as:

$$SO_4^{2-} + 1.33CH_2 + 0.66H_2O \rightarrow H_2S + 1.33CO_2 + 2OH^- \quad (7)$$

indicating that CO_2 is a by-product of BSR. The $\delta^{13}C$ of oxidized organic matter (−22 to −35‰) is significantly different from atmospheric CO_2 (−7‰) and marine carbonate (−5 to +2‰), suggesting that BSR should affect the $\delta^{13}C$ of dissolved HCO_3^- in thermal spring waters.

The $\delta^{13}C$ values of total dissolved inorganic C are plotted versus the calculated % biological cycling in Fig. 13. There is a rough trend of decreasing $\delta^{13}C$ with increasing biological cycling, as would be expected. However, there is significant scatter in these data. The $\delta^{13}C$ values of total dissolved inorganic C from thermal spring waters are plotted versus total alkalinity in Fig. 14. Thermal springs with low alkalinity (< 100 mg/l) have $\delta^{13}C$ values that vary from +5 to −25‰. In contrast, at high alkalinity, the $\delta^{13}C$ values of springs converge to a value around −5‰. This relationship may be explained by mixing of two C sources, where high alkalinity represents waters with HCO_3 derived from dissolution of carbonate rock, whereas low alkalinity waters represent more of an organic source. Thus dissolution of carbonate rock may be masking any relation between $\delta^{13}C$ and biological cycling of SO_4.

These results have implications for ^{14}C dating of thermal spring waters. As illustrated in Fig. 14, the DIC of thermal springs have a $\delta^{13}C$ value consistent with an organic origin only at low alkalinity (< 100 mg/l). Even then, some low alkalinity springs have $\delta^{13}C$ values that indicate C derived from dissolution of carbonate rock (i.e. 'dead' C). All the springs with alkalinity above 100 mg/l have $\delta^{13}C_{HCO_3}$ values consistent with dissolution of carbonate rocks. This shows that ^{14}C age dating of thermal springs will probably give artificially old ages due to the addition of 'dead' C.

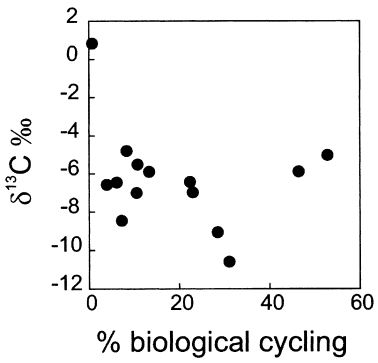

Fig. 13. $\delta^{13}C_{HCO_3}$ versus calculated % of biological cycling. There is little correlation contrary to what might be expected.

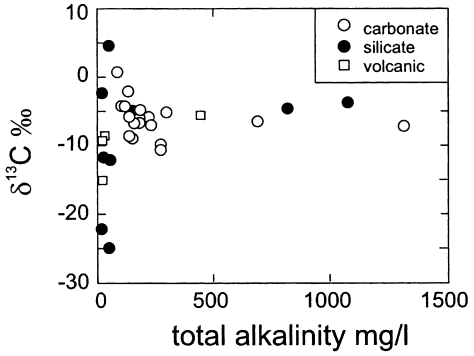

Fig. 14. $\delta^{13}C_{HCO_3}$ versus total alkalinity indicating a significant contribution of dissolved carbonates to high alkalinity waters, thus masking any possible relation between $\delta^{13}C_{HCO_3}$ and biological cycling in Fig. 13.

7. Summary and conclusions

Despite the highly variable geological setting of thermal systems within the Canadian Cordillera, some basic generalizations may be made about the controls on the geochemistry of the thermal springs, and presumably similar springs elsewhere. The thermal springs in this study originate as meteoric water that circulates through the crust to obtain heat and chemical components. A comparison of historical records indicates that the chemistry of thermal springs appears to be constant through time, suggesting that water–rock interactions in these systems are either steady state kinetic processes, or that chemical compositions develop equilibrium within the host rock. The comparison of mineral stability with water compositions presented here indicates that the activities of major cations may be adequately explained by equilibrium reactions with common rock forming minerals and alteration products. In contrast, the major anion SO_4 is largely influenced by the biological activity in the springs.

Sulfate in carbonate hosted springs is mainly derived from dissolution of evaporite minerals. This SO_4 is reduced by bacteria, causing the production of HS^-. The loss of HS^- from the system appears to be minor, instead it is reoxidized to SO_4 as the spring water ascends to the surface. Assuming that 100% of the O used in oxidizing HS^- to SO_4 is from H_2O, then the amount of SO_4 that has been reduced and reoxidized (% biological cycling) varies from 0 to 53%. The % biological cycling would be even greater if some O is obtained from atmospheric O_2. There is an inverse relationship between the % biological cycling of SO_4 and the concentration of SO_4, indicating that SO_4 is

not a limiting nutrient in these hydrothermal systems. These results are consistent with models for the formation of Eocene hydrothermal ore deposits in the southeastern Canadian Cordillera. Beaudoin et al. (1992) suggest that Eocene extensional faults channeled mineralizing fluids towards upper crustal levels where they mixed with S-rich meteoric waters circulating down to depths of 6 km. Grasby and Hutcheon (1999) calculate circulation depths of 2.5 to 5 km for thermal springs in the southern Cordillera. Thus modern thermal systems are capable of bringing bacterially reduced S to depths where ore formation occurs.

In low-alkalinity thermal springs, HCO_3 may be derived from either dissolution of carbonate minerals or oxidized organic matter. However, for high-alkalinity springs (>100 mg/l), HCO_3 is derived from carbonate dissolution. This limits the ability to use ^{14}C dating methods for waters from these springs.

Acknowledgements

Special thanks go to those who assisted in trying to find, and sample, the various thermal springs: Teresa Grasby, Marian Johnson, Jeff Nazerchuck, Robert Grasby, Rhonda Waller and Ann-Lise Norman. Many people helped by providing directions to hard to find springs, particularly Glen Woodsworth. Parks Canada allowed access to many springs and facilities. Funding for this project was provided by research grants to I.H. and H.R.K. from the Natural Science and Research Council of Canada. Reviews by Jake Lowenstern and Chris Ferrar helped improve this manuscript. Geological Survey of Canada contribution 1999042.

References

Abercrombie, H., 1988. Water–rock interaction during diagenesis and thermal recovery, Cold Lake, Alta. Ph.D. thesis, University of Calgary, Canada.

Armstrong, R.L., 1988. Mesozoic and early Cenozoic magmatic evolution of the Canadian Cordillera. GSA Special Paper 218, 55–91.

Arnorsson, S., 1975. Application of the silica geothermometer in low temperature hydrothermal areas in Iceland. Am. J. Sci. 275, 763–784.

Beaudoin, G., Roddick, J.C., Sangster, D.F., 1992. Eocene age for Ag–Pb–Zn–Au vein and replacement deposits of the Kokanee Range, BC. Can. J. Earth Sci. 29, 3–14.

Brown, G.W., Berman, R.G., Perkins, E.H., 1988. GEØ-CALC: a0 software package for rapid calculation of stable pressure-temperature-activity phase diagrams using an IBM or compatible personal computer. Comput. Geosci. 14, 279–289.

Chiba, H., Sakai, H., 1985. Oxygen isotope exchange rate between dissolved sulphate and water at hydrothermal temperatures. Geochem. Cosmochim. Acta 49, 993–1000.

Clapp, C.H., 1913. Sharp Point hotspring, Vancouver Island. Geol. Surv. Canada Summary Report, 80–83.

Clark, I.D., Fritz, P., Souther, J.G., 1982. Isotope hydrology and geothermometry of the Mt. Meager geothermal area. Can. J. Earth Sci. 19, 1454–1473.

Claypool, G.E., Holser, W.T., Kaplan, I.R., Sakai, M., Zak, I., 1980. The age curves of sulfur and oxygen isotopes in marine sulfate and their mutual interpretation. Chem. Geol. 28, 199–260.

Coleman, M.L., Shepard, T.J., Durham, J.J., Rouse, J.D., Moore, G.R., 1982. Reduction of water with zinc for hydrogen isotope analysis. Anal. Chem. 54, 993–995.

Craig, H., 1963. The isotopic geochemistry of water and carbon in geothermal areas. In: Tongiorgi, E. (Ed.), Nuclear Geology on Geothermal Areas. Consiglio Nazionale delle Ricerche, Laboratorio di Geologia Nucleare, Pisa, pp. 17–53.

Crandall, J.T., Sadlier-Brown, T.L., 1976. Data on geothermal areas Cordilleran Yukon, Northwest Territories, and adjacent British Columbia, Canada. Department of Energy Mines and Resources, Open File No. 78-1, Ottawa, Canada.

Dansgaard, W., 1964. Stable isotopes in precipitation. Tellus 16, 436–468.

Elworthy, R.T., 1918. Mineral springs of Canada, Part II: the chemical character of some Canadian mineral springs. Canada Mines Branch Bulletin No. 20, 173 pp.

Environment Canada, 1983. Sampling for Water Quality. Inland Waters Directorate, Water Resources Branch, Water Survey of Canada, Ottawa.

Epstein, S., Mayeda, T.K., 1953. Variation of ^{18}O content of waters from natural sources. Geochim. Cosmochim. Acta 4, 213–224.

Fournier, R.O., Truesdell, A.H., 1973. An empirical Na–K–Ca chemical geothermometer for natural waters. Geochim. Cosmochim. Acta 37, 1255–1275.

Gabrielse, H., Yorath, C.J., 1991. Geology of the Cordilleran Orogen in Canada. Geol. Surv. Canada, Geology of Canada Series, v. 4 (GSA Geology of North America G-2), 844 pp.

Garrels, R.M., Mackenzie, F.T., 1967. Origin of the chemical compositions of some springs and lakes: equilibrium concepts in natural water systems. Am. Chem. Soc. Adv. Chem. Ser. 67, 222–242.

Ghomshei, M.M., Clark, I.D., 1993. Oxygen and hydrogen in deep thermal waters from the south Meager Creek geothermal area. BC Geothermics 22, 79–89.

Grasby, S.E., Hutcheon I., 1999. Controls on the distribution of thermal springs in southern Alberta and British Columbia. Submitted for publication.

Kacandes, G.H., Grandstaff, D.E., 1989. Differences between geothermal and experimentally derived fluids: how well do hydrothermal experiments model the composition of geothermal reservoir fluids? . Geochim. Cosmochim. Acta 53, 343–358.

Kelly, D.P., 1982. Biochemistry of the chemolithotrophic oxidation of inorganic sulphur. Philos. Trans. R. Soc. London, Ser. B 298, 499–528.

Kharaka, Y.K., Mariner, R.H., 1988. Chemical geotherm-

ometers and their application to formation waters from sedimentary basins. In: Naeser, N.D., McCulloh, T. (Eds.), Thermal History of Sedimentary Basins. Springer Verlag, New York, pp. 99–117.

Krouse, H.R., 1976. Sulphur isotope variations in thermal and mineral waters. In: Cadek, J., Paces, T. (Eds.), Proceedings International Symposium on Water–Rock Interaction, pp. 343–347.

Krouse, H.R., 1980. Sulphur isotopes in our environment. In: Fritz, P., Fontes, J. (Eds.), Handbook of Environmental Isotope Geochemistry, The Terrestrial Environment, vol. 1. Elsevier, Amsterdam, pp. 22–44.

Krouse, H.R., Cook, F.D., Sasaki, A., Smejkal, V., 1970. Microbiological isotope fractionation in springs of western Canada. In: Proceedings of the International Conference on Mass Spectroscopy, pp. 629–639.

Lewis, T.J., Souther, J.G., 1978. Meager Mountain, BC: a possible geothermal energy resource. Earth Physics Branch, Energy Mines and Resources Canada, Geothermal Series No. 9.

Lloyd, R.M., 1967. Oxygen-18 composition of oceanic sulphate. Science 156, 1228–1231.

Mazor, E., van Everdingen, R.O., Krouse, H.R., 1983. Noble gas evidence for geothermal activity in a karstic terrain: Rocky Mountains, Canada. Geochim. Cosmochim. Acta 47, 1111–1115.

McCrea, J.M., 1950. On the isotopic chemistry of carbonates and a paleotemperature scale. J. Chem. Phys. 18, 848–857.

McCready, R.G.L., Krouse, H.R., 1980. Sulphur isotope fractionation by *Desulfovibrio vulgaris* during metabolism of $BaSO_4$. Geomicrobiol. J. 2, 55–62.

Michelot, J., Dotsika, E., Fytikas, M., 1993. A hydrochemical and isotopic study of thermal waters on Lesbos Island, Greece. Geothermics 22, 91–99.

Mizutani, Y., Rafter, T.A., 1969. Oxygen isotopic composition of sulphates, 3. Oxygen isotopic fractionation in the bisulfate ion-water system. NZ J. Sci. 12, 54–59.

Nesbitt, B.E., Muehlenbachs, K., 1995. Geochemical studies of the origins and effects of synorogenic crustal fluids in the southern Omineca Belt of British Columbia, Canada. Geol. Soc. Am. Bull. 107, 1033–1050.

Nesbitt, B.E., Muehlenbachs, K., Murowchick, J.B., 1989. Genetic implications of stable isotope characteristics of mesothermal Au deposits and related Sb and Hg deposits in the Canadian Cordillera. Econ. Geol. 84, 1489–1506.

Phillips, R.J., 1994. Isotope hydrology and aqueous geochemistry of selected British Columbia hotsprings. M.Sc. thesis, University of Ottawa, Canada.

Shakur, A., 1982. ^{34}S and ^{18}O variations in terrestrial sulphates. Ph.D. thesis, University of Calgary, Canada.

Smejkal, V., Cook, F.D., Krouse, H.R., 1971. Studies of sulphur and carbon isotope fractionation with microorganisms isolated from springs of western Canada. Geochim. Cosmochim. Acta 35, 787–800.

Souther, J.G., 1976. Geothermal power, the canadian potential. Geosci. Can. 3, 14–20.

Souther, J.G., 1992. Geothermal energy. In: Gabrielse, H., Yorath. C.J. (Eds.), Geology of the Cordilleran Orogen in Canada. 787–792. Geol. Surv. Canada, Geology of Canada Series, 4 (Geological Society of America, Geology of North America, G-2).

Souther, J.G., Halstead, E.C., 1973. Mineral and thermal waters of Canada. Geol. Surv. Can. Pap. 73-18.

Sturchio, N.C., Arehart, G.B., Sultan, M., Sano, Y., AboKamar, Y., Sayed, M., 1996. Composition and origin of thermal waters in the Gulf of Suez area, Egypt. Appl. Geochem. 11, 471–479.

van Everdingen, R.O., 1972. Thermal and Mineral Springs in the Southern Rocky Mountains of Canada. Water Management Service, Environment Canada.

van Everdingen, R.O., 1984. Dirt-water events at Rocky Mountain Hot Springs and their correlation with other short-lived phenomena. Can. J. Earth Sci. 21, 997–1007.

van Everdingen, R.O., Shakur, M.A., Krouse, H.R., 1982. Isotope geochemistry of dissolved, precipitated, airborne and fallout sulphur species associated with springs near Paige Mountain, Norman Range, Northwest Territ. Can. J. Earth Sci. 19, 1385–1407.

van Stempvoort, D.R., Krouse, H.R., 1994. Controls of ^{18}O in sulfate: review of geochemistry of sulfide oxidation. In: Alpers, C.N., Blowes, D.W. (Eds.), ACS Symp. Series 550, pp. 446–480.

Wang, Y., Shpeyzer, G.M., 1997. Genesis of thermal groundwaters from Siping'an district, China. Appl. Geochem. 12, 437–445.

Wheeler, J.O., 1961. Whitehorse map area, Yukon Territ. 105D. Geol. Surv. Can. Mem. 312.

White, D.E., 1975. Thermal waters of volcanic origin. Geol. Soc. Am. Bull. 68, 1637–1658.

Wiwchar, B., Perkins, E.H., Gunter, W.D., 1988. SOLMINEQ.88 PC/SHELL Manual. Alberta Research Council, Oil sands and hydrocarbon recovery department.

Worden, R.H., Smalley, P.C., Oxtoby, N.H., 1995. Gas souring by thermochemical sulfate reduction at 140°C. Am. Assoc. Petrol. Geol. Bull. 79, 854–863.

Yanagisawa, F., Sakai, H., 1983. Precipitation of SO_2 for sulphur isotope ratio measurements by thermal decomposition of $BaSO_4$–V_2O_5–SiO_2 mixtures. Anal. Chem. 55, 985–987.

Yonge, C.J., Goldberg, L., Krouse, H.R., 1989. An isotope study of water bodies along a traverse of southwestern Canada. J. Hydrol. 106, 245–255.